# Blind Identification of SIMO Systems and Simultaneous Estimation of Multiple Time Delays From HOS-Based Inverse Filter Criteria

Chong-Yung Chi, *Senior Member, IEEE*, Ching-Yung Chen, Chii-Horng Chen, Chih-Chun Feng, *Member, IEEE*, and Chun-Hsien Peng

***Abstract*—Higher order statistics-based inverse filter criteria (IFC) have been effectively used for blind equalization of single-input multiple-output (SIMO) systems. Recently, Chi and Chen reported a relationship between the unknown SIMO system and the optimum equalizer designed by the IFC for finite signal-to-noise ratio (SNR). In this paper, based on this relationship, an iterative fast Fourier transform (FFT)-based nonparametric blind system identification (BSI) algorithm and an FFT-based multiple-time-delay estimation (MTDE) algorithm are proposed with a given set of non-Gaussian measurements. The proposed BSI algorithm allows the unknown SIMO system to have common subchannel zeros, and its performance (estimation accuracy) is superior to that of the conventional IFC-based methods. The proposed MTDE algorithm can simultaneously estimate all the $(P-1)$ time delays (with respect to a reference sensor) with space diversity of sensors exploited; therefore, its performance (estimation accuracy) is robust to the nonuniform distribution of SNRs of $P \geq 2$ sensors (due to channel fading). Some simulation results are presented to support the efficacy of the proposed BSI algorithm and MTDE algorithm.**

***Index Terms*—Blind system identification, cumulant-based inverse filter criteria, higher order statistics, time delay estimation.**

## I. Introduction

BLIND identification of single-input multiple-output (SIMO) systems deals with the problem of estimating a $P \times 1$ linear time-invariant (LTI) system, which is denoted by $\mathbf{h}[n] = (h_1[n], h_2[n], \ldots, h_P[n])^T$ (where the superscript "$T$" denotes vector or matrix transposition), with only the $P \times 1$ output vector measurements $\mathbf{y}[n] = (y_1[n], y_2[n], \ldots, y_P[n])^T, n = 0, 1, \ldots, N-1$, generated from the following convolutional model:

$$\mathbf{y}[n] = \mathbf{h}[n] * u[n] + \mathbf{w}[n] = \sum_{k=-\infty}^{\infty} \mathbf{h}[k] u[n-k] + \mathbf{w}[n] \quad (1)$$

Manuscript received August 12, 2002; revised October 8, 2003. This work was supported by the National Science Council under Grants NSC 89-2213-E007-032 and NSC 91-2219-E007-014. Part of this work was presented at IEEE Workshop on Statistical Signal Processing, Singapore, August 6–8, 2001. The associate editor coordinating the review of this paper and approving it for publication was Dr. Alex C. Cot.

C.-Y. Chi and C.-H. Peng are with the Department of Electrical Engineering and Institute of Communications Engineering, National Tsing Hua University, Hsinchu, Taiwan 30013, R.O.C. (e-mail: cychi@ee.nthu.edu.tw; d905610@oz.nthu.edu.tw).

C.-Y. Chen and C.-C. Feng are with the Computer and Communications Research Laboratories, Industrial Technology Research Institute, Hsinchu, Taiwan, R.O.C. (e-mail: danchen@itri.org.tw; ccfeng@sunplus.com.tw).

C.-H. Chen is with ADMtek Incorporated, Hsinchu, Taiwan, R.O.C. (e-mail: chiihorng.chen@infineon.com).

Digital Object Identifier 10.1109/TSP.2004.834219

where $u[n]$ is the scalar driving input, and $\mathbf{w}[n] = (w_1[n], w_2[n], \ldots, w_P[n])^T$ is the $P \times 1$ vector noise. The SIMO system model given by (1) is typically based on the following assumptions that are also made in this paper.

- $\mathcal{A}1$) The driving input $u[n]$ is a zero-mean, independent identically distributed (i.i.d.), non-Gaussian random process with variance $\sigma_u^2 = E\{|u[n]|^2\}$.
- $\mathcal{A}2$) The SIMO system $\mathbf{h}[n]$ is a finite impulse response (FIR) system with frequency response [discrete-time Fourier transform (DTFT) of $\mathbf{h}[n]$] $\boldsymbol{H}(\omega) \neq \mathbf{0}_P$ ($P \times 1$ zero vector) for all $-\pi < \omega \leq \pi$.
- $\mathcal{A}3$) The noise $\mathbf{w}[n]$ is zero-mean spatially uncorrelated Gaussian and statistically independent of $u[n]$.

The problem of blind SIMO system identification arises in diverse science and engineering areas where multiple sensors are applied such as wireless communications with multiple receiving antennas (or antenna array) and time delay estimation (TDE). It also arises when multirate signal processing is involved such as fractionally spaced equalization of communication channels [1]–[3].

The existing approaches to blind identification of SIMO systems basically include the maximum likelihood (ML)-based methods and the moment-based methods. The ML estimator, which is derived from a presumed probability density function of measurements, has the optimal asymptotic performance at the expense of extraordinary computational complexity that makes it unfavorable in practical applications. Reduction of computational complexity of the ML estimator, however, is possible; see [4] for further details. On the other hand, the moment-based methods, typically with lower complexity than the ML estimator, exploit either second-order statistics (SOS) or higher order statistics (HOS) [5] of measurements to estimate the unknown system. Since Tong *et al.* proposed [6] a pioneering work of blind SIMO system identification using SOS, many SOS-based SIMO blind system identification (BSI) methods, which are often referred to as subspace methods, have been reported over the last decade, including the noise subspace (NS) method [7], [8], the least-squares smoothing method [9], [10], and the linear prediction method [11]. These subspace methods have the attractive property that an estimate of the FIR system of interest can often be obtained in a closed form by optimizing a quadratic cost function [3]. However, some of these methods require the knowledge of the system order, and their performance is sensitive to the system order

mismatch [3]. Furthermore, a common identifiability condition referred to as the channel disparity condition, which is required by these subspace methods, is that the subchannels must be coprime (i.e., the subchannels have no common zeros), and these methods tend to fail when this condition is nearly violated [12], [13]. Recently, the NS method [7] that was modified by Ali *et al.* [14] was shown to be robust in the presence of common subchannel zeros and the system order overestimation errors by virtue of exploiting the transmitter redundancy through the use of a trailing zero precoder. However, the use of a precoding procedure will limit applications of the modified subspace method, as reported in [14]. As a consequence, the subspace methods are usually not very flexible due to the restrictions mentioned above.

The HOS-based SIMO BSI methods basically comprise three broad classes [15]: equation error-based methods [16], [17], fitting error-based methods [18], [19], and inverse filter criteria (IFC)-based methods [20], [21]. Assuming that the system order is known in advance, the equation error-based methods proposed by Hatzinakos and Nikias [16] and by Brooks and Nikias [17] estimate the system by the least-squares solution from certain theoretical linear equations formed by channel parameters and statistics of $\mathbf{y}[n]$. These methods generally provide a unique but not very accurate solution for the system impulse response, and their performance is also sensitive to the modeling error. The fitting error-based methods proposed by Swami *et al.* [18] and by Tugnait [19] estimate $\mathbf{h}[n]$ by matching the model-based statistics with the estimated data-based statistics, which involve the estimation of a great amount of cumulants [5] and result in a nonlinear optimization problem where a good initial estimate is needed because of potential local minima of the cost function used. Therefore, in addition to higher complexity for cumulants estimation than for correlations estimation, large sample size is required to reduce the variance of estimated cumulants (such as sample cumulants). The IFC-based methods proposed by Tugnait [20] and by Chi *et al.* [21] find the equalizer by maximizing (or minimizing) a certain objective function of the equalizer output, which generally results in a nonlinear optimization problem. Then, the system estimate is simply obtained by cross-correlation of the equalizer output (input signal estimate) and the noisy system output $\mathbf{y}[n]$ with no need for order determination. Unlike the fitting error-based methods, the IFC-based methods usually involve computation of only one normalized cumulant, and thus, they are significantly released from the high variance issue induced by estimation of cumulants. However, the obtained system estimate using the conventional IFC-based methods has bias [22] due to the presence of noise in $\mathbf{y}[n]$ and the estimation error of the input signal estimate (the equalizer output).

Recently, Chi and Chen [23] established a relationship between the linear minimum mean-square error (MMSE) equalizer and the optimum equalizer associated with the IFC reported in [20] and [21] for finite signal-to-noise ratio (SNR). Based on this relationship, a novel iterative fast Fourier transform (FFT)-based nonparametric SIMO BSI algorithm that allows the subchannels to have common zeros and exhibits better performance than the conventional IFC-based methods is proposed in this paper.

On the other hand, the estimation of time delay(s) between the measurements received by two (or more) sensors is crucial in many signal processing areas such as direction of arrival and range estimation in sonar, radar, and geophysics, etc. The conventional methods using SOS [24], [25] estimate a single time delay with the associated two sensor measurements at a time (instead of simultaneous estimation of multiple time delays) by finding the peak location of the cross-correlation function of the associated two sensor measurements. These methods may yield ambiguous results when the noise components among sensors are spatially correlated or coherent. Techniques based on HOS [26]–[30] have been reported to avoid such ambiguous results. Among them, the performance of the integrated polyspectrum-based method proposed by Ye and Tugnait [30] has been proven to asymptotically approach the Cramér–Rao (CR) lower bound.

By the fact that the signal model for the TDE problem can be formulated as an SIMO model and the fact that the complete information of all the time delays is contained in the phase of the SIMO system, a novel FFT-based TDE algorithm, which is also based on the relationship between the linear MMSE equalizer and the optimum equalizer associated with the IFC mentioned above, is proposed for simultaneous estimation of all the time delays (with respect to a reference sensor) with space diversity of sensors exploited. Therefore, its performance is insensitive to the nonuniform distribution of SNRs of sensors due to channel fading.

The remaining parts of this paper are organized as follows. In Section II, the relationship between the SIMO system and the optimum equalizer designed by the IFC is presented. Then, the proposed BSI algorithm and multiple-time-delay estimation (MTDE) algorithm are presented in Sections III and IV, respectively. Some simulation results are provided in Section V to verify the efficacy of the proposed algorithms, and some conclusions are drawn in Section VI.

## II. Relationship Between the Unknown System and the Optimum Equalizer Designed by the IFC

For ease of later use, let us define the SNRs associated with $y_i[n]$ and $\mathbf{y}[n]$ given by (1), respectively, as follows:

$$\text{SNR}_i = \frac{E\{|y_i[n] - w_i[n]|^2\}}{E\{|w_i[n]|^2\}} \tag{2}$$

$$\text{SNR} = \frac{E\{\|\mathbf{y}[n] - \mathbf{w}[n]\|^2\}}{E\{\|\mathbf{w}[n]\|^2\}} \tag{3}$$

where $\|\mathbf{a}\|$ denotes the Euclidean norm of vector $\mathbf{a}$. Note that $\text{SNR}_i$ denotes the SNR of the $i$th subchannel (or sensor), SNR denotes the overall SNR, and that there exist many different distributions of $\{\text{SNR}_i, i = 1, 2, \ldots, P\}$ corresponding to the same SNR.

Processing the measurements $\mathbf{y}[n]$ given by (1) by a $P$-input single-output equalizer denoted by $\mathbf{v}[n] = (v_1[n], v_2[n], \ldots, v_P[n])^T$ yields the (scalar) equalized signal

$$e[n] = \mathbf{v}^T[n] * \mathbf{y}[n] = g[n] * u[n] + \tilde{w}[n] \tag{4}$$

where $\tilde{w}[n] = \mathbf{v}^T[n] * \mathbf{w}[n]$ corresponds to the noise part in $e[n]$, and

$$g[n] = \mathbf{v}^T[n] * \mathbf{h}[n] \tag{5}$$

is the scalar overall system (after equalization). The well-known linear MMSE equalizer, which is denoted by $\mathbf{v}_{\mathrm{MMSE}}[n]$, is a *nonblind* equalizer that minimizes the mean square error (MSE) $E\{|\hat{u}[n] - u[n]|^2\}$, where $\hat{u}[n] = \mathbf{v}_{\mathrm{MMSE}}^T[n] * \mathbf{y}[n]$. Note that either system information or training phase is needed to obtain the linear MMSE equalizer $\mathbf{v}_{\mathrm{MMSE}}[n]$.

On the other hand, with no need for system information and training phase, the equalizer $\mathbf{v}[n]$ can be obtained by maximizing the following HOS-based IFC [20]–[23]

$$J_{p,q}(\mathbf{v}[n]) = J_{p,q}(e[n]) = \frac{|C_{p,q}\{e[n]\}|}{|C_{1,1}\{e[n]\}|^{(p+q)/2}} \tag{6}$$

where $p+q \geq 3$, $C_{1,1}\{e[n]\} = E\{|e[n]|^2\}$, and

$$C_{p,q}\{e[n]\} = \mathrm{cum}\{\underbrace{e[n], \ldots, e[n]}_{p \text{ terms}}, \underbrace{e^*[n], \ldots, e^*[n]}_{q \text{ terms}}\} \tag{7}$$

denotes the $(p+q)$th-order joint cumulant of $p$ $e[n]$'s and $q$ $e^*[n]$'s in which the superscript '*' denotes complex conjugation. Since $J_{p,q}(\mathbf{v}[n])$ is a highly nonlinear function of $\mathbf{v}[n]$, iterative gradient-type optimization algorithms are required to find the maximum of $J_{p,q}(\mathbf{v}[n])$ and the associated $\mathbf{v}[n]$.

It has been shown [20] that, under the noise-free condition (infinite SNR) and the assumptions $\mathcal{A}1$) and $\mathcal{A}2$), the optimum equalizer $\mathbf{v}[n]$ associated with $J_{p,q}$ with sufficient length results in perfect recovery of the driving input, i.e., the associated equalized signal

$$e[n] = \alpha u[n - \tau] \tag{8}$$

where $\alpha \neq 0$ is an unknown scale factor, and $\tau$ is an unknown time delay. As reported by Tugnait [20], the unknown SIMO system $\mathbf{h}[n]$ can be accordingly estimated as

$$\hat{\mathbf{h}}[n] = \frac{E\{\mathbf{y}[m+n]e^*[m]\}}{E\{|e[m]|^2\}} \tag{9}$$

which is referred to as the input–output cross-correlation (IOCC) method (which is also a conventional IFC-based BSI method) for convenience. One can easily see, from (8) and (9), that $\hat{\mathbf{h}}[n] = (1/\alpha) \cdot \mathbf{h}[n + \tau]$ (perfect system identification) for the case of infinite SNR. On the other hand, for finite SNR, the optimum equalized signal $e[n]$, in the sense of maximizing $J_{p,q}$, is an MMSE-like estimate of the driving input $u[n]$ (see [15, ch. 8] for the detailed discussion), and the channel estimation accuracy of the IOCC method that ignores noise effects is degraded. Nevertheless, the channel-induced phase distortion is completely removed by the optimum equalizer $\mathbf{v}[n]$, as described in the following fact [23]:

*Fact 1:* The optimum overall system $g[n] \neq 0$ [see (5)] associated with $J_{p,q}$ for finite SNR is a linear phase system, i.e.,

$$G(\omega) = |G(\omega)|e^{j(\omega\tau + \kappa)} \tag{10}$$

where $\tau$ and $\kappa$ are an integer and a real constant, respectively. ■

With noise effects taken into account, we further propose an SIMO BSI method based on a relationship between the system $\mathbf{h}[n]$ and the equalizer $\mathbf{v}[n]$ associated with $J_{p,p}$ for any SNR where only the case of $p = q$ for $J_{p,q}$ is considered in this paper. The relationship has been reported by Chi and Chen (see [23, Prop. 2]) for MIMO systems, which is summarized as follows.

*Fact 2:* With sufficient length of the equalizer $\mathbf{v}[n]$, the system $\mathbf{h}[n]$ is related to the equalizer $\mathbf{v}[n]$ associated with $J_{p,p}$ for any SNR via the following relationship:

$$G_p(\omega) \cdot \boldsymbol{H}^*(\omega) = \beta \cdot \boldsymbol{\mathcal{S}}_y^T(\omega)\boldsymbol{V}(\omega) \tag{11}$$

where $\boldsymbol{\mathcal{S}}_y(\omega)$ (the power-spectral matrix of $\mathbf{y}[n]$) is the DTFT of the autocorrelation function of $\mathbf{y}[n]$, which is defined as

$$\begin{aligned}\mathbf{R}_y[k] &= E\{\mathbf{y}[n]\mathbf{y}^H[n-k]\} \\ &= \sigma_u^2 \cdot \mathbf{h}[k] * \mathbf{h}^H[-k] + E\{\mathbf{w}[n]\mathbf{w}^H[n-k]\}\end{aligned} \tag{12}$$

(where the superscript "$H$" denotes complex conjugate of vector or matrix transposition), $G_p(\omega)$ is the DTFT of

$$g_p[n] = g^p[n](g^*[n])^{p-1} \tag{13}$$

and

$$\beta = \frac{C_{p,p}\{e[n]\}}{C_{1,1}\{e[n]\} \cdot C_{p,p}\{u[n]\}} = \frac{\sum_n |g[n]|^{2p}}{E\{|e[n]|^2\}} > 0 \tag{14}$$

is a real constant. ■

Note that not only the optimum equalizer $\mathbf{v}[n]$ associated with the maximum of $J_{p,p}(\mathbf{v}[n])$ satisfies (11) but all the other local optimum $\mathbf{v}[n]$'s and the trivial solution $\mathbf{v}[n] = \mathbf{0}_P$ as well. However, only the former is the equalizer of interest. Let us conclude this section with the following two remarks.

- R1) Fact 2 also holds true when the Gaussian noise vector $\mathbf{w}[n]$ is spatially correlated and temporally colored [23].
- R2) In practice, sample cumulants $\hat{C}_{p,p}\{e[n]\}$ and $\hat{C}_{1,1}\{e[n]\}$, which are consistent estimates of $C_{p,p}\{e[n]\}$ and $C_{1,1}\{e[n]\}$ regardless of SNR, are used to compute $J_{p,p}(e[n])$; therefore, the optimum $\mathbf{v}[n]$ obtained by maximizing $J_{p,p}(\mathbf{v}[n])$ is also consistent for finite SNR [32]. However, the IOCC method [see (9)] is not a consistent estimator of $\mathbf{h}[n]$ for finite SNR (with larger bias for smaller SNR) [15].

## III. Blind Identification of SIMO Systems

It can be observed, from (11), as stated in Fact 2, that given the optimum equalizer $\mathbf{v}[n]$ obtained using $J_{p,p}(\mathbf{v}[n])$ given by (6) and the power-spectral matrix $\boldsymbol{\mathcal{S}}_y(\omega)$ using an existing multichannel power spectral estimator, the system $\mathbf{h}[n]$ can be estimated by solving (11) if the solution for $\mathbf{h}[n]$ of the highly nonlinear equation (11) is unique over the class that the overall system is linear phase (motivated by Fact 1). Meanwhile, noise effects embedded in $\boldsymbol{\mathcal{S}}_y(\omega)$ [see (12)] and $\mathbf{v}[n]$ (through the denominator $E\{|e[n]|^2\}$ of $J_{p,p}(\mathbf{v}[n])$) can also be taken into account in the estimation of $\mathbf{h}[n]$, regardless of the value of

SNR. Prior to presenting the algorithm for obtaining $\mathbf{h}[n]$, let us present an analysis about the solution set of $\mathbf{h}[n]$ that is solved from the highly nonlinear equation (11) with the following constraint.

C1) The overall system $g[n] \neq 0$ be linear phase.

### *A. Analysis About the Systems Solved from (11) Under Constraint C1)*

With (11), the system $\mathbf{h}[n]$ can be solved up to a linear phase ambiguity as revealed in the following property.

*Property 1:* Any SIMO system

$$\boldsymbol{H}'(\omega) = \boldsymbol{H}(\omega) \cdot e^{j(\omega\tau+\kappa)} \tag{15}$$

for any integer $\tau$ and real $\kappa$ satisfies the relationship given by (11). ■

See Appendix A for the proof of Property 1. Property 1 and C1) imply that $g[n]$ can be zero phase, which further leads to the following property about the system $g_p[n]$ given by (13).

*Property 2:* Assume that $g[n] \neq 0$ is zero-phase and that

$\mathcal{A}4$) the number of zeros of $G(\omega)$ on the unit circle is finite.

Then, the associated system $g_p[n] \neq 0$ given by (13) is a positive definite sequence, i.e., $G_p(\omega) > 0, \forall -\pi < \omega \leq \pi$. ■

The proof of Property 2 is given in Appendix B. Next, let us present the following property regarding the solution set of $\mathbf{h}[n]$ from (11) under constraint C1).

*Property 3:* The system $\boldsymbol{H}(\omega)$ can be identified up to a linear phase ambiguity by solving (11) assuming that $g[n] \neq 0$ is zero-phase and satisfies $\mathcal{A}4$). ■

See Appendix C for the proof of Property 3 in which Property 2 is needed. Property 3 implies that the solution of (11) under the constraint C1) and the assumption $\mathcal{A}4$) is the true system $\boldsymbol{H}(\omega)$ (without bias) except for a time delay (due to a linear phase ambiguity) as long as the true $\mathbf{v}[n]$ and $\boldsymbol{\mathcal{S}}_y(\omega)$ are given. Therefore, Property 3 and R2) imply the following remark:

R3) The channel estimate $\hat{\mathbf{h}}[n]$ solved from (11) under constraint C1) and the assumption $\mathcal{A}4$) is consistent for finite SNR if an estimate $\hat{\boldsymbol{\mathcal{S}}}_y(\omega)$ can be obtained using a consistent multichannel power spectral estimator. With our experience, assumption $\mathcal{A}4$) generally holds true in practical applications and is never an issue in the design of BSI algorithms.

Again, one can see, from (5) and (13), that the left-hand side of (11) is a highly nonlinear function of $\mathbf{h}[n]$, implying that a closed-form solution of (11) for $\mathbf{h}[n]$ is almost formidable under constraint C1). Next, let us present an iterative FFT-based nonparametric algorithm for estimating $\mathbf{h}[n]$ under the constraint C1).

### *B. Algorithm for Obtaining the System Estimate from (11) Under Constraint C1)*

Let $\boldsymbol{a}_k$ and $\boldsymbol{b}_k$ be $P \times 1$ vectors defined as

$$\boldsymbol{a}_k = G_p[k]\boldsymbol{H}^*[k], \quad k = 0, 1, \ldots, \mathcal{L}-1 \tag{16}$$

$$\boldsymbol{b}_k = \boldsymbol{\mathcal{S}}_y^T[k]\boldsymbol{V}[k], \quad k = 0, 1, \ldots, \mathcal{L}-1 \tag{17}$$

where $G_p[k]$, $\boldsymbol{H}[k]$, $\boldsymbol{\mathcal{S}}_y[k]$, and $\boldsymbol{V}[k]$, $k = 0, 1, \ldots, \mathcal{L}-1$ denote the $\mathcal{L}$-point discrete Fourier transforms (DFTs) of $g_p[n]$, $\mathbf{h}[n]$, $\mathbf{R}_y[n]$, and $\mathbf{v}[n]$, respectively. Then, according to the relationship given by (11), one can obtain

$$\mathbf{a} = \beta\mathbf{b} \tag{18}$$

where $\mathbf{a} = (\boldsymbol{a}_0^T, \boldsymbol{a}_1^T, \ldots, \boldsymbol{a}_{\mathcal{L}-1}^T)^T$ and $\mathbf{b} = (\boldsymbol{b}_0^T, \boldsymbol{b}_1^T, \ldots, \boldsymbol{b}_{\mathcal{L}-1}^T)^T$, and $\beta$ is given by (14). Let us emphasize that the positive constant $\beta$ in (18) is unknown, and this implies that either $\beta$ must be estimated together with the estimation of $\mathbf{h}[n]$ or its role must be virtual during the estimation of $\mathbf{h}[n]$. Thus, let us present an algorithm based on (18) without involving estimation of $\beta$ for the estimation of $\mathbf{h}[n]$.

Equations (16)–(18) reveal that the true system $\boldsymbol{H}(\omega)$ is the one such that the resultant vector $\mathbf{a}$ is equal to the vector $\mathbf{b}$, except for a real positive scale factor. Thus, $\boldsymbol{H}(\omega)$ at $\omega = \omega_k = 2\pi k/\mathcal{L}, k = 0, 1, \ldots, \mathcal{L}-1$ can be estimated by maximizing

$$\mathcal{C}(\boldsymbol{H}[k]) \triangleq \frac{\mathrm{Re}\{\mathbf{a}^H\mathbf{b}\}}{\|\mathbf{a}\| \cdot \|\mathbf{b}\|} \tag{19}$$

where $\mathrm{Re}\{\nu\}$ denotes the real part of scalar $\nu$. Note that $-1 \leq \mathcal{C}(\boldsymbol{H}[k]) = \mathcal{C}(\alpha\boldsymbol{H}[k]) \leq 1$ for any $\alpha \neq 0$ and that $\mathcal{C}(\boldsymbol{H}[k]) = 1$ if and only if $\mathbf{a}$ is equal to the vector $\mathbf{b}$ up to a real positive scalar.

However, it is almost impossible to obtain the gradient $\partial\mathcal{C}(\boldsymbol{H}[k])/\partial\boldsymbol{H}[k]$ because $\mathcal{C}(\boldsymbol{H}[k])$ is a highly nonlinear function of $\boldsymbol{H}[k]$; therefore, gradient-based optimization methods are not considered for finding the maximum of $\mathcal{C}(\boldsymbol{H}[k])$. Instead, an iterative FFT-based BSI algorithm is proposed to obtain the estimate of $\boldsymbol{H}[k], k = 0, 1, \ldots, \mathcal{L}-1$, which can be thought of as a numerical optimization approach, as described below.

*BSI Algorithm:*

Step 1) *Blind Deconvolution and Power-Spectral Matrix Estimation:*

With finite data $\mathbf{y}[n]$, obtain the equalizer estimate $\hat{\mathbf{v}}[n]$ associated with $J_{p,p}(\hat{\mathbf{v}}[n])$, and compute its $\mathcal{L}$-point FFT $\hat{\boldsymbol{V}}[k]$, $k = 0, 1, \ldots, \mathcal{L}-1$. Obtain the power-spectral matrix estimate $\hat{\boldsymbol{\mathcal{S}}}_y[k]$, $k = 0, 1, \ldots, \mathcal{L}-1$, using a multichannel power spectral estimator. Form the vector $\hat{\boldsymbol{b}}_k$ via $\hat{\boldsymbol{\mathcal{S}}}_y[k]$ and $\hat{\boldsymbol{V}}[k], k = 0, 1, \ldots, \mathcal{L}-1$, according to (17).

Step 2) *System Identification:*

T1) Set the iteration number $i = 0$ and the initial condition $\boldsymbol{H}^{(0)}[k]$, $k = 0, 1, \ldots, \mathcal{L}-1$. Obtain $\hat{G}^{(0)}[k] = \hat{\boldsymbol{V}}^T[k]\boldsymbol{H}^{(0)}[k]$, followed by its $\mathcal{L}$-point inverse FFT $\hat{g}^{(0)}[n]$.

T2) Update $i$ by $i+1$. Update $\hat{g}^{(i-1)}[n] = g[n]$, where

$$g[n] = \frac{1}{2}\left(\hat{g}^{(i-1)}[n] + \hat{g}^{(i-1)}[-n]\right)^* \quad \text{(zero phase)} \tag{20}$$

and then obtain

$$\boldsymbol{H}^{(i)}[k] = \left(\frac{1}{\hat{G}_p^{(i-1)}[k]} \cdot \hat{\boldsymbol{b}}_k\right)^*$$

$$k = 0, 1, \ldots, \mathcal{L}-1 \quad \text{[by (16) and (18)]}$$

where $\hat{G}_p^{(i-1)}[k]$ is the $\mathcal{L}$-point FFT of $\hat{g}_p^{(i-1)}[n]$ obtained by (13). Normalize $\boldsymbol{H}^{(i)}[k]$ such that $\sum_k ||\boldsymbol{H}^{(i)}[k]||^2 = 1$.

T3) Obtain $\hat{G}^{(i)}[k] = \hat{\boldsymbol{V}}^T[k]\boldsymbol{H}^{(i)}[k]$ [by (5)] followed by its $\mathcal{L}$-point inverse FFT $\hat{g}^{(i)}[n]$. If $\mathcal{C}(\boldsymbol{H}^{(i)}[k]) > \mathcal{C}(\boldsymbol{H}^{(i-1)}[k])$, go to T4). Otherwise, compute $\Delta\boldsymbol{H}[k] = \boldsymbol{H}^{(i)}[k] - \boldsymbol{H}^{(i-1)}[k]$, $k = 0, 1, \ldots, \mathcal{L}-1$, and update $\boldsymbol{H}^{(i)}[k]$ via

$$\boldsymbol{H}^{(i)}[k] = \boldsymbol{H}^{(i-1)}[k] + \mu \cdot \Delta\boldsymbol{H}[k], \quad k = 0, 1, \ldots, \mathcal{L}-1$$

where the step size $\mu$ is chosen such that $\mathcal{C}(\boldsymbol{H}^{(i)}[k]) > \mathcal{C}(\boldsymbol{H}^{(i-1)}[k])$. Normalize $\boldsymbol{H}^{(i)}[k]$ such that $\sum_k ||\boldsymbol{H}^{(i)}[k]||^2 = 1$.

T4) If

$$\frac{\mathcal{C}\left(\boldsymbol{H}^{(i)}[k]\right) - \mathcal{C}\left(\boldsymbol{H}^{(i-1)}[k]\right)}{\left|\mathcal{C}\left(\boldsymbol{H}^{(i-1)}[k]\right)\right|} > \epsilon$$

where $\epsilon$ is a preassigned convergence tolerance, then go to T2); otherwise, the frequency response estimate $\hat{\boldsymbol{H}}(\omega) = \boldsymbol{H}^{(i)}(\omega)$ at $\omega = 2\pi k/\mathcal{L}$ for $k = 0, 1, \ldots, \mathcal{L}-1$ and its $\mathcal{L}$-point inverse FFT $\hat{\mathbf{h}}[n]$ are obtained.

Several worthy remarks regarding the proposed BSI algorithm are as follows.

R4) In Step 1, the equalizer estimate $\hat{\mathbf{v}}[n]$ associated with $J_{p,p}(\hat{\mathbf{v}}[n])$ can be efficiently obtained using Chi and Chen's fast iterative gradient-type algorithm (see [23, Alg. 2]), and the existing AR spectral estimators, such as the multichannel Levinson recursion algorithm [31], can be employed to estimate $\boldsymbol{\mathcal{S}}_y[k]$.

R5) In Step 2, the local convergence is guaranteed because $\mathcal{C}(\boldsymbol{H}^{(i)}[k])$ is upper bounded by unity, and its value is increased at each iteration before convergence. The closer to unity the convergent $\mathcal{C}(\boldsymbol{H}^{(i)}[k])$, the more reliable the obtained system estimate. Empirically, with the estimate of $\hat{\mathbf{h}}[n]$ obtained by (9) (Tugnait's IOCC method) for the initial condition $\boldsymbol{H}^{(0)}[k]$ in T1) of Step 2, the convergent $\mathcal{C}(\boldsymbol{H}^{(i)}[k]) = 1$ is always obtained.

R6) In T3) of Step 2, the step size $\mu$ can be chosen sequentially from the finite sequence $\{1/2, 1/4, \ldots, 1/(2^\eta), -1, -1/2, -1/4, \ldots, -1/(2^\eta)\}$ until $\mathcal{C}(\boldsymbol{H}^{(i)}[k]) > \mathcal{C}(\boldsymbol{H}^{(i-1)}[k])$ whenever $\mu$ is needed at each iteration, where $\eta$ is a preassigned positive integer.

R7) Prior information of an upper bound of the system order is needed. The FFT size $\mathcal{L}$ should be chosen to be larger than the upper bound of the order of $\mathbf{h}[n]$ such that aliasing effects on the resultant $\hat{\mathbf{h}}[n]$ are negligible. Surely, the larger the FFT size, the larger the computational load of the proposed BSI algorithm, whereas the estimation error of the resultant $\hat{\mathbf{h}}[n]$ is almost the same. If the true system is an infinite impulse response (IIR) system, a finite-length approximation of $\mathbf{h}[n]$ will be obtained by the proposed BSI algorithm. Furthermore, the system $\mathbf{h}[n]$ is allowed to have common subchannel zeros (i.e., regardless of whether the channel disparity condition is satisfied).

R8) Noise effects have been taken into account in the estimation of $\mathbf{v}[n]$ and the power-spectral matrix $\boldsymbol{\mathcal{S}}_y[k]$ in Step 1. Let us emphasize that the larger data length $N$, the better the estimates $\hat{\mathbf{v}}[n]$ and $\hat{\boldsymbol{\mathcal{S}}}_y[k]$, regardless of the value of SNR [see R2) and R3)], which implies that the better approximation $\hat{\mathbf{h}}[n]$ to $\mathbf{h}[n]$ will be obtained for larger $N$, except for an unknown time delay (by Property 3) and a scale factor (due to $\mathcal{C}(\boldsymbol{H}[k]) = \mathcal{C}(\alpha\boldsymbol{H}[k])$), whereas the associated overall system $\hat{g}[n]$ is guaranteed to be zero phase due to (20) in T2) of Step 2. Moreover, as long as the SNR is higher than a threshold, the estimation error of the obtained estimate $\hat{\mathbf{h}}[n]$ basically reaches a floor which is lower for larger $N$ by R3).

Next, let us turn to the estimation of multiple time delays that is also based on the relationship given by (11).

## IV. Simultaneous Estimation of Multiple Time Delays

Assume that the measurements $\mathbf{y}[n] = (y_1[n], y_2[n], \ldots, y_P[n])^T, n = 0, 1, \ldots, N-1$, are measured from $P$ ($\geq 2$) spatially separated sensors that satisfy

$$\begin{cases} y_1[n] = x[n] + w_1[n] \\ y_i[n] = x[n] * c_i[n] + w_i[n], \quad i = 2, 3, \ldots, P \end{cases} \tag{21}$$

where $x[n]$ is the source signal (could be colored), and $c_i[n], i \in \{2, 3, \ldots, P\}$ is an LTI system of frequency response

$$C_i(\omega) = A_i e^{-j\omega d_i} \tag{22}$$

where $A_i$ and $d_i, i = 2, 3, \ldots, P$ are (real or complex) gains and real numbers, respectively, and $\mathbf{w}[n] = (w_1[n], w_2[n], \ldots, w_P[n])^T$ is a $P \times 1$ vector noise whose components can be spatially correlated and temporally colored. Note that $C_i(\omega)$ given by (22) is called the (scaled) ideal delay system of $d_i$ sample delay, even if $d_i$ is not an integer. Therefore, for notational convenience, let us rewrite the signal model given by (21) as

$$\mathbf{y}[n] = (x[n], A_2 x[n-d_2], \ldots, A_P x[n-d_P])^T + \mathbf{w}[n]. \tag{23}$$

The goal is to estimate all the $(P-1)$ time delays $\{d_2, d_3, \ldots, d_P\}$ simultaneously from the measurements $\mathbf{y}[n]$. Note that the signal model given by (23) consists of a colored signal that passes through flat fading (frequency-flat) channels and impinges on an array of sensors. Multipath TDE with only two sensor measurements can be found in [33]–[35].

Let us further assume that the source signal $x[n]$ is stationary colored non-Gaussian and can be modeled as

$$x[n] = \sum_{k=-\infty}^{\infty} \tilde{h}[k]u[n-k] \tag{24}$$

where $\tilde{h}[n]$ is a stable LTI system, and $u[n]$ is a zero-mean, i.i.d. non-Gaussian random sequence. Substituting (24) into (23) gives rise to an SIMO system model, as given by (1), with

$$\mathbf{h}[n] = (\tilde{h}[n], A_2\tilde{h}[n-d_2], \ldots, A_P\tilde{h}[n-d_P])^T. \quad (25)$$

Note that all of the $P$ subchannels of the SIMO system $\mathbf{h}[n]$ given by (25) have the same zeros. The time delays $\{d_2, d_3, \ldots, d_P\}$ can be extracted from the SIMO system $\mathbf{h}[n]$, which can be estimated from the measurements $\mathbf{y}[n]$ ahead of time by means of blind SIMO system identification methods such as the proposed BSI algorithm. In light of the specific form of $\mathbf{h}[n]$ given by (25) and the fact that the phase information of $\mathbf{h}[n]$ is sufficient for retrieving the multiple time delays, the estimation of $\{d_2, d_3, \ldots, d_P\}$ can be quite efficient, as illustrated below.

The specific form of $\mathbf{h}[n]$ given by (25) leads to

$$\angle\{\boldsymbol{H}(\omega)\} = (\angle\{\tilde{H}(\omega)\}, \angle\{\tilde{H}(\omega)\} + \theta_2 - \omega d_2, \ldots \angle\{\tilde{H}(\omega)\} + \theta_P - \omega d_P)^T \quad (26)$$

where $\angle\{\boldsymbol{H}(\omega)\}$ denotes the phase response of $\boldsymbol{H}(\omega)$, $\tilde{H}(\omega)$ is the DTFT of $\tilde{h}[n]$, and the constant phase $\theta_i$ denotes the phase of $A_i$. On the other hand, because $\beta$ is real and positive, it can be easily seen, from the key relationship given by (11) [which holds true as the Gaussian noise vector $\mathbf{w}[n]$ is spatially correlated and temporally colored by R1)], that

$$\begin{aligned}\angle\{\boldsymbol{H}(\omega)\} &= \angle\left\{\boldsymbol{\mathcal{S}}_y^H(\omega)\boldsymbol{V}^*(\omega)\right\} - \angle\{G_p^*(\omega)\} \\ &= (\Phi_1(\omega) - \angle\{G_p^*(\omega)\}, \Phi_2(\omega) - \angle\{G_p^*(\omega)\}, \ldots \\ &\quad \Phi_P(\omega) - \angle\{G_p^*(\omega)\})^T \end{aligned} \quad (27)$$

where

$$(\Phi_1(\omega), \Phi_2(\omega), \ldots, \Phi_P(\omega))^T \triangleq \angle\left\{\boldsymbol{\mathcal{S}}_y^H(\omega)\boldsymbol{V}^*(\omega)\right\}. \quad (28)$$

By subtracting $\angle\{\tilde{H}(\omega)\}$ and $(\Phi_1(\omega) - \angle\{G_p^*(\omega)\})$ (i.e., the first element of $\angle\{\boldsymbol{H}(\omega)\}$) from each element of $\angle\{\boldsymbol{H}(\omega)\}$ given by (26) and (27), respectively, one can obtain

$$\begin{aligned}&(0, \Phi_2(\omega) - \Phi_1(\omega), \ldots, \Phi_P(\omega) - \Phi_1(\omega))^T \\ &\qquad = (0, \theta_2 - \omega d_2, \ldots, \theta_P - \omega d_P)^T. \end{aligned} \quad (29)$$

Then, letting

$$\begin{aligned}\boldsymbol{F}(\omega) &= (F_1(\omega), F_2(\omega), \ldots, F_P(\omega))^T \\ &= \left(1, e^{j[\Phi_2(\omega) - \Phi_1(\omega)]}, \ldots, e^{j[\Phi_P(\omega) - \Phi_1(\omega)]}\right)^T \end{aligned} \quad (30)$$

simply leads to

$$\boldsymbol{F}(\omega) = \left(1, e^{j(\theta_2 - \omega d_2)}, \ldots, e^{j(\theta_P - \omega d_P)}\right)^T. \quad (31)$$

It can be found that the inverse DTFT of $F_i(\omega)$, $i \in \{2, 3, \ldots, P\}$ is

$$f_i[n] = e^{j\theta_i} \cdot \frac{\sin(\pi(n - d_i))}{\pi(n - d_i)} \quad (32)$$

which can be thought of as a sequence obtained by sampling a continuous-time signal

$$f_i(t) = e^{j\theta_i} \cdot \frac{\sin(\pi(t - d_i T)/T)}{\pi(t - d_i T)/T} \quad (33)$$

with sampling period $T$. Note that $|f_i(t)| \leq |f_i(d_i T)| = 1, \forall t$ and, thus, $d_i$ can be estimated by

$$\hat{d}_i = \frac{1}{T}\arg\{\max_t |f_i(t)|\}. \quad (34)$$

Approximately, $d_i$ can be estimated within an acceptable resolution via sampling $f_i(t)$ with a higher sampling period, as described below. Consider another sequence $b_i[n]$, which is obtained from sampling $f_i(t)$ with sampling rate $T/K$, i.e., $b_i[n] = f_i(t = nT/K)$, where $K$ is a positive integer such that $Kd_i$ apporximates an integer. Then, it can be shown that $|b_i[n]| \leq |b_i[Kd_i]|, \forall n$, which implies that $d_i$ can be estimated by finding the time index associated with the maximum value of $|b_i[n]|$. Because $b_i[n]$ (with sampling period $T/K$) is essentially an interpolated version of $f_i[n]$ (with sampling period $T$), the above idea can be efficiently implemented by calculating the zero-padded FFT, as reported in [29]. Given $F_i[k] = F_i(\omega = 2\pi k/\mathcal{L}), k = 0, 1, \ldots, \mathcal{L} - 1$, let $\bar{\mathcal{L}} = K\mathcal{L}$, and define

$$B_i[k] = \begin{cases} F_i[k], & 0 \leq k \leq (\mathcal{L}/2) - 1 \\ F_i[k + \mathcal{L} - \bar{\mathcal{L}}], & \bar{\mathcal{L}} - (\mathcal{L}/2) \leq k \leq \bar{\mathcal{L}} - 1 \\ 0, & \text{otherwise} \end{cases} \quad (35)$$

Then, the $\bar{\mathcal{L}}$-point inverse DFT of $B_i[k], b_i[n], n = 0, 1, \ldots, \bar{\mathcal{L}} - 1$ is exactly the interpolated version of $f_i[n], n = 0, 1, \ldots, \mathcal{L} - 1$. Moreover, let us define

$$\begin{aligned}\bar{b}_i[n] &= b_i[((n - \bar{\mathcal{L}}/2) \text{ modulo } \bar{\mathcal{L}})] \\ n &= 0, 1, \ldots, \bar{\mathcal{L}} - 1. \quad \text{(i.e., circular shift of } b_i[n]\text{)}. \end{aligned} \quad (36)$$

Then, the time delays can be estimated as

$$\hat{d}_i = \frac{n_i - \bar{\mathcal{L}}/2}{K}, \quad i = 2, 3, \ldots, P \quad (37)$$

where

$$n_i = \arg\{\max\{|\bar{b}_i[n]|, 0 \leq n \leq \bar{\mathcal{L}} - 1\}\}. \quad (38)$$

Note that (37) means that the resolution of the estimated time delays is $1/K$. The larger the $K$, the better the estimation accuracy of $\hat{d}_i$'s, especially for the case of noninteger time delays.

The proposed FFT-based MTDE algorithm is summarized as follows.

*MTDE Algorithm:*

- S1) With finite data $\mathbf{y}[n]$, obtain the equalizer estimate $\hat{\mathbf{v}}[n]$ associated with $J_{p,p}(\hat{\mathbf{v}}[n])$, and compute its $\mathcal{L}$-point FFT $\hat{\boldsymbol{V}}[k]$, where $k = 0, 1, \ldots, \mathcal{L}-1$. Obtain the power-spectral matrix estimate $\hat{\boldsymbol{\mathcal{S}}}_y[k]$, $k = 0, 1, \ldots, \mathcal{L}-1$ using a multichannel power spectral estimator.
- S2) Compute $\hat{\boldsymbol{F}}[k], k = 0, 1, \ldots, \mathcal{L}-1$, according to (30) and (28), and then compute $\overline{b}_i[n]$ for $i = 2, 3, \ldots, P$ [by (35) and (36)].
- S3) Estimate $\{d_2, d_3, \ldots, d_P\}$ by (37) and (38).

Let us conclude this section with the following two remarks.

- R9) Unlike the conventional TDE methods (which estimate a single time delay with the associated two sensor measurements at a time), the proposed MTDE algorithm simultaneously processes all the sensor measurements. In other words, the space diversity of multiple sensors has been exploited by the proposed MTDE algorithm, implying that its performance is robust to the nonuniform distribution of $\{\text{SNR}_i, i = 1, 2, \ldots, P\}$ resulting from channel fading, as long as the overall SNR keeps the same.
- R10) The proposed MTDE algorithm can also be employed to estimate each time delay using the associated two sensor measurements as the conventional TDE methods. In other words, the MTDE algorithm reduces to a single time delay estimation algorithm, which is referred to as the "MTDE-1 algorithm" for distinction from the MTDE algorithm using all the sensor measurements. However, the performance of the MTDE-1 algorithm is inferior to that of the MTDE algorithm because the space diversity is not exploited [see R9)] by the former.

## V. Simulation Results

In this section, some simulation results are provided to justify the efficacy of the proposed BSI algorithm (to be presented in Part A with Examples 1–3 below) and MTDE algorithm (to be presented in Part B with Example 4 below) for blind identification of SIMO systems and simultaneous estimation of multiple time delays, respectively. In each of the examples, 100 independent runs were performed for different data length $N$ and different SNR [defined by (3)], and all the cumulants needed were replaced by the associated sample cumulants [5].

### A. Blind Identification of SIMO Systems

This part considers the estimation of single-input three-output $(P = 3)$ systems. The driving input $u[n]$ was assumed to be a zero-mean i.i.d. binary sequence of $\{+1, -1\}$ with equal probability. The data $\mathbf{y}[n]$ were synthesized using (1) with real spatially independent and temporally white Gaussian noise $\mathbf{w}[n]$. The synthetic data $\mathbf{y}[n]$ were then processed by the proposed BSI algorithm with the following settings. In Step 1 of the BSI algorithm, a $3 \times 1$ causal FIR filter of order equal to 7 was used for the equalizer $\mathbf{v}[n]$ associated with the IFC $J_{2,2}(\mathbf{v}[n])$ $(p = q = 2)$, and an AR multichannel power spectral estimator of order equal to 4 was used to estimate the power-spectral matrix of $\mathbf{y}[n]$. In Step 2 of the BSI algorithm, the FFT size $\mathcal{L} = 64$, the convergence tolerance $\epsilon = 10^{-10}$, and the parameter $\eta = 10$ to choose the parameter $\mu$ [see R6)] were used.

Let $\hat{h}_i[n; r]$ denote the estimate of the $i$th subchannel $h_i[n]$ (the $i$th entry of $\mathbf{h}[n]$) obtained at the $r$th run with both the time delay and scale factor removed. Since the order of each system considered in the following examples is either smaller than or approximately equal to 15, only 16 coefficients of each estimate $\hat{h}_i[n; r]$ $(n = 0 \sim 15)$ were used for the performance evaluation of the proposed BSI algorithm. Specifically, the normalized mean square error (NMSE) associated with $h_i[n]$ defined as

$$\text{NMSE}_i = \frac{1}{100} \cdot \frac{\sum_{r=1}^{100} \sum_{n=0}^{15} |\hat{h}_i[n; r] - h_i[n]|^2}{\sum_n |h_i[n]|^2} \tag{39}$$

was computed for all the subchannels and then averaged to obtain the overall NMSE (ONMSE) [20]

$$\text{ONMSE} = \frac{1}{P} \sum_{i=1}^{P} \text{NMSE}_i \tag{40}$$

which was used as the performance index.

On the other hand, for comparison, the HOS-based IOCC method [20] and the SOS-based NS method [7] were also employed to estimate $\mathbf{h}[n]$ with the same simulation data. Note that both the proposed BSI algorithm and the IOCC method only require an upper bound of the system order, whereas the NS method requires the exact system order. Therefore, in Examples 1 and 2 below, where the systems are FIR, the NS method with system order assumed to be known was used to attain its best performance. Next, let us turn to the first example.

*Example 1—FIR System without Common Subchannel Zeros:* In this example, a $3 \times 1$ MA(3) system (taken from [20]) with the transfer function

$$\boldsymbol{H}(z) = \begin{bmatrix} 0.7426 + 0.7426z^{-2} \\ 0.4456z^{-1} + 0.7426z^{-2} \\ 0.8911z^{-2} + 0.5941z^{-3} \end{bmatrix} \triangleq \boldsymbol{H}_{\text{ex1}}(z) \tag{41}$$

is considered. Fig. 1 shows the simulation results (ONMSEs versus SNR) associated with the proposed BSI algorithm (indicated by "Proposed BSI"), the IOCC method (indicated by "IOCC"), the NS method with the system order assumed to be 3 (indicated by "NS (order $= 3$)"), and the NS method with the system order assumed to be 4 (indicated by "NS (order $= 4$)"). One can observe, from this figure, that the NS method with system order assumed to be 4 (i.e., order over-determined by 1 only) totally failed, verifying the fact that it has a high sensitivity to system order mismatch. One can also observe, from Fig. 1(a) and (b), that the proposed BSI algorithm always outperforms the IOCC method and that both of them perform well with the estimation error (ONMSEs) basically reaching a floor for SNR $\geq 5$ dB (a threshold), and that the floor is lower for larger $N$, as described in R8). On the other hand, the NS method (with the order exactly known) performs much better than the

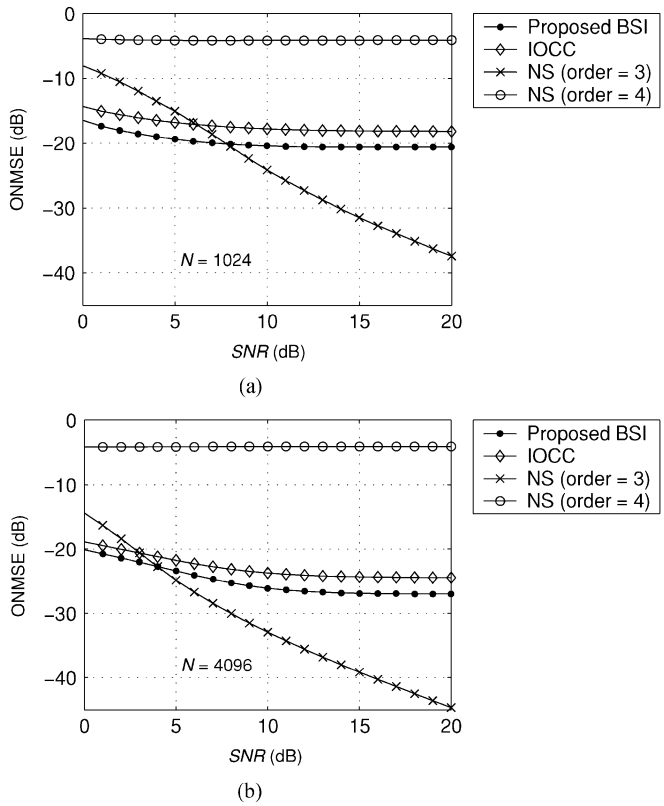


Fig. 1. Simulation results of Example 1. Plots of ONMSEs versus SNR associated with the proposed BSI algorithm, the IOCC method, and the NS method, respectively, for data length (a) $N = 1024$ and (b) $N = 4096$.

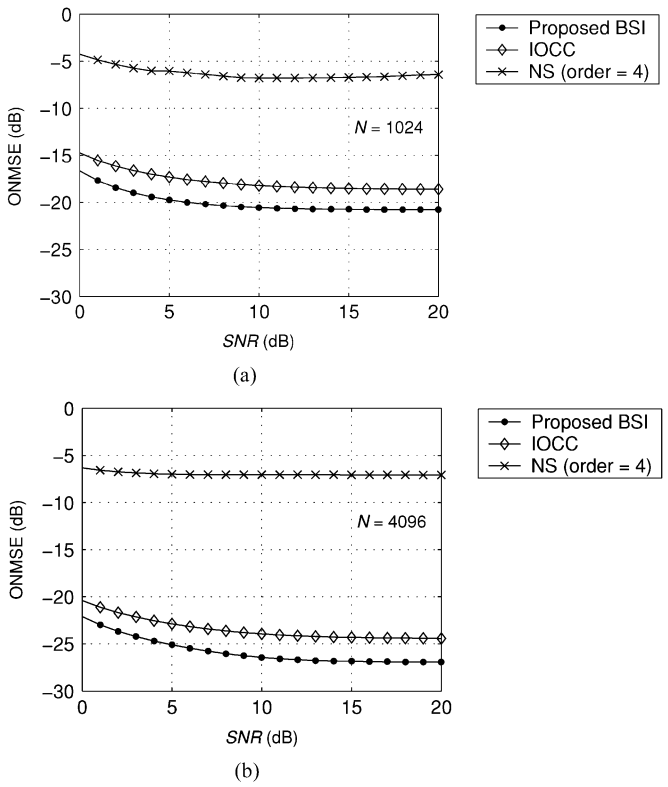


Fig. 2. Simulation results of Example 2. Plots of ONMSEs versus SNR associated with the proposed BSI algorithm, the IOCC method, and the NS method, respectively, for data length (a) $N = 1024$ and (b) $N = 4096$.

proposed BSI algorithm and the IOCC method for high SNR, and its performance significantly improves with the increase of SNR.

*Example 2—FIR System with Common Subchannel Zeros:* This example considers the estimation of a $3 \times 1$ MA(4) system $\boldsymbol{H}(z) = (1 - 0.5z^{-1}) \cdot \boldsymbol{H}_{\rm ex1}(z)$, where $\boldsymbol{H}_{\rm ex}1(z)$ is given by (41). Obviously, the system has a common subchannel zero at $z = 0.5$ and, thus, does not satisfy the channel disparity condition. Fig. 2 shows the simulation results obtained using the proposed BSI algorithm, the IOCC method, and the NS method with system order equal to the true order of $\boldsymbol{H}(z)$. One can see, from this figure, that both the proposed BSI algorithm and the IOCC method perform well, whereas the NS method failed in this example due to the violation of channel disparity condition. Moreover, the performance of the proposed BSI algorithm, again, is always superior to that of the IOCC method.

*Example 3—IIR System with Common Subchannel Poles:* This example considers the estimation of a $3 \times 1$ system $\boldsymbol{H}(z) = (1 - 0.5z^{-1})^{-1} \cdot \boldsymbol{H}_{\rm ex1}(z)$ with a common subchannel pole at $z = 0.5$. Note that $\boldsymbol{H}(z)$ itself is an IIR system, and so, its length is actually equal to infinity. The IIR system $\boldsymbol{H}(z)$ was approximated by FIR systems with length equal to 3, 4, and 5 for the NS method in the simulation. The simulation results corresponding to those shown in Fig. 1 are shown in Fig. 3. One can see, from Fig. 3, that the NS method failed because the system to be identified is not an FIR system with well-defined order and that both the proposed BSI algorithm and the IOCC method perform well, and the performance of the former is superior to that of the latter.

In summary, the above three examples demonstrate the efficacy of the proposed BSI algorithm for different SNRs, data lengths, and channel models, and typically only 2–5 iterations in Step 2 were spent in obtaining $\hat{\mathbf{h}}[n]$ in the above simulation results.

### B. Simultaneous Estimation of Multiple Time Delays

This part considers the problem of simultaneously estimating two time delays ($d_2$ and $d_3$) of a non-Gaussian source signal impinging on three sensors (i.e., $P = 3$) using the proposed MTDE algorithm. For comparison, $d_2$ and $d_3$ are also separately estimated by the MTDE-1 algorithm [see R10)] as well as Ye and Tugnait's integrated bispectrum based time delay estimator (IBBTDE) [30] with the associated two sensor measurements used. That is, with respect to the first sensor, $d_2$ and $d_3$ are also separately estimated by the MTDE-1 algorithm and the IBBTDE, respectively, with the data sets $\{y_1[n], y_2[n]\}$ and $\{y_1[n], y_3[n]\}$ in the following example, respectively.

*Example 4:* The source signal $x[n]$ was assumed to be a zero-mean, i.i.d. one-sided exponentially distributed sequence, as assumed in the simulations in [30]. The noise sequence $w_1[n]$ (in the first sensor) was assumed to be a zero-mean colored Gaussian sequence generated as the output of the following MA(1) system:

$$H_w(z) = 1 + 0.8z^{-1}$$

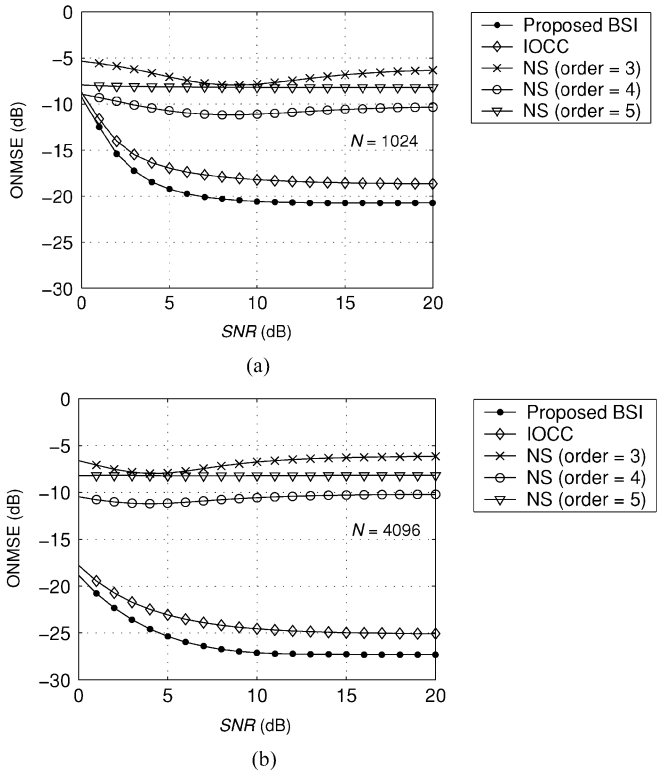


Fig. 3. Simulation results of Example 3. Plots of ONMSEs versus SNR associated with the proposed BSI algorithm, the IOCC method, and the NS method, respectively, for data length (a) $N = 1024$ and (b) $N = 4096$.

driven by a real white Gaussian sequence. The noise sequence $w_2[n] = w_1[n]$ (in the second sensor) was perfectly correlated with $w_1[n]$, and the noise sequence $w_3[n]$ (in the third sensor) was correlated with $w_1[n]$ by $w_3[n] = a(w_1[n] - w_1[n-6])$, where $a$ was chosen such that $E[|w_i[n]|^2]$ for $i = 1, 2, 3$ are the same (i.e., equal noise power for the three sensors). The data $\mathbf{y}[n]$ were synthesized according to (23) with the two time delays $\{d_2 = 2.5, d_3 = 11.4\}$ and two gains $\{A_2, A_3\}$ given as follows.

Case A: $A_2 = A_3 = 1$ (i.e., $\text{SNR}_1 = \text{SNR}_2 = \text{SNR}_3$).
Case B: $A_2 = 3$ and $A_3 = -2$ (i.e., $\text{SNR}_1 < \text{SNR}_3 = 4\text{SNR}_1 < \text{SNR}_2 = 9\text{SNR}_1$).

The synthetic data $\mathbf{y}[n]$ were then processed by the proposed MTDE algorithm with the following settings: a $3 \times 1$ causal FIR filter (or a $2 \times 1$ causal FIR filter) of order equal to 9 for the equalizer $\mathbf{v}[n]$ associated with the IFC $J_{2,2}(\mathbf{v}[n])$ $(p = q = 2)$, an AR multichannel power spectral estimator of order equal to 12 for power-spectral matrix estimation, the FFT size $\mathcal{L} = 128$, and $K = 100$. On the other hand, for the IBBTDE, the entire record of each independent run was divided into 128-sample nonoverlapping segments for the integrated bispectrum estimation, and the initial condition required for phase matching was obtained by the method of [29] with a resolution of $1/128$.

The simulation results for Case A and Case B are displayed in Figs. 4 and 5, respectively. These figures show the root-mean-square errors (RMSEs) and means of the time delay estimates $\hat{d}_2$ and $\hat{d}_3$ associated with the proposed MTDE algorithm (denoted by "□" with all the sensor measurements used), the MTDE-1 algorithm (denoted by "○"), and the IBBTDE (denoted by "×")

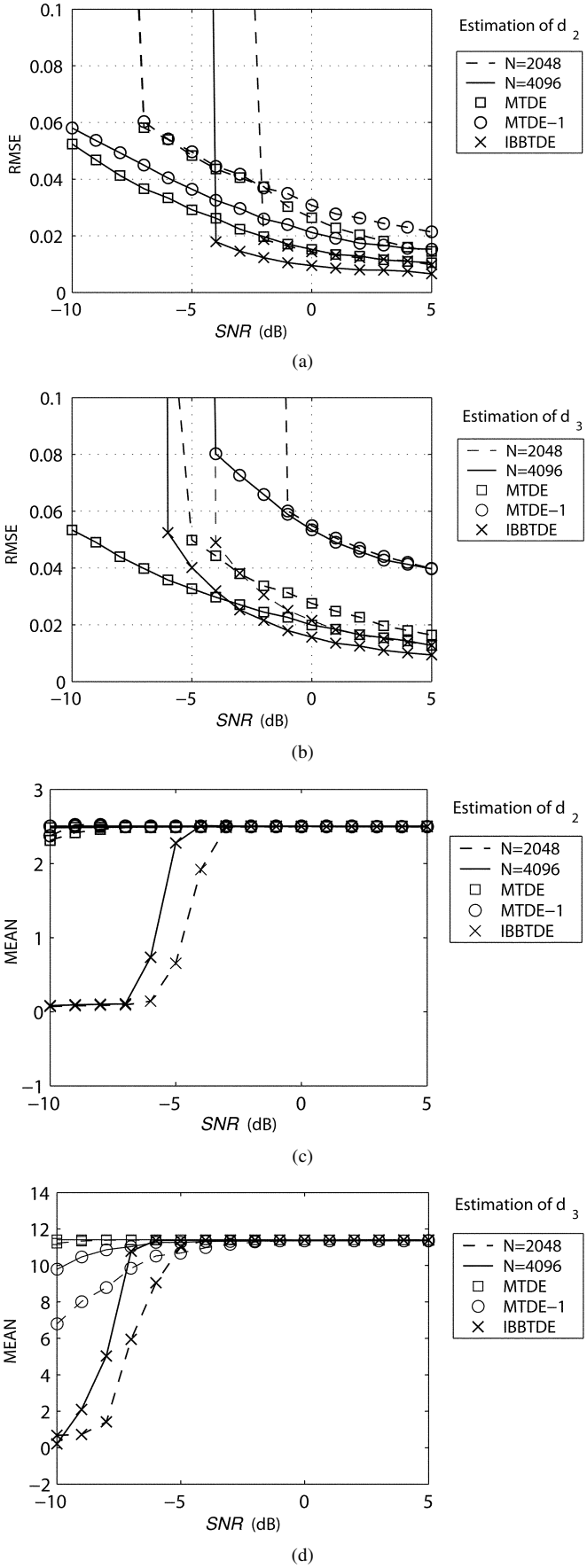


Fig. 4. Simulation results of Case A of Example 4 for estimating two time delays of $d_2 = 2.5$ and $d_3 = 11.4$. (a) and (b) Plots of the RMSEs of $\hat{d}_2$ and $\hat{d}_3$, respectively. (c) and (d) Plots of the means of $\hat{d}_2$ and $\hat{d}_3$, respectively.

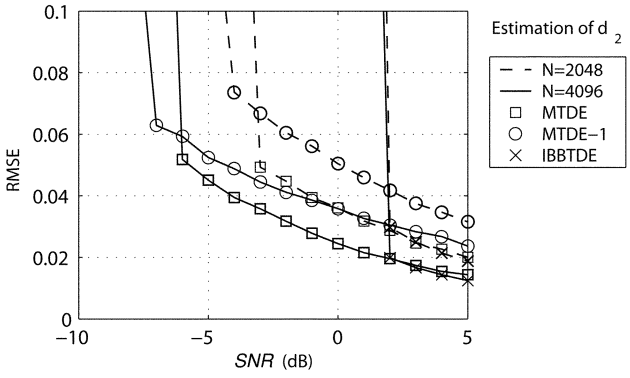


(a)

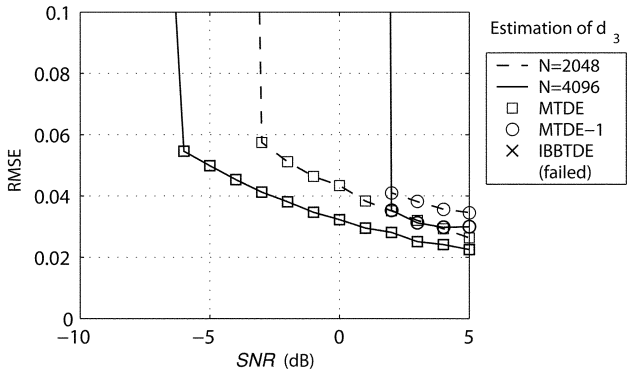


(b)

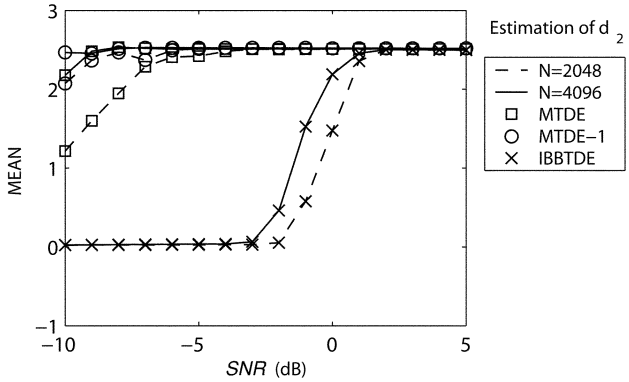


(c)

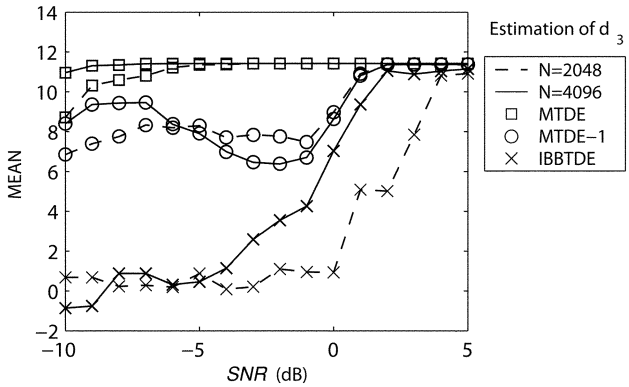


(d)

Fig. 5. Simulation results of Case B of Example 4 for estimating two time delays of $d_2 = 2.5$ and $d_3 = 11.4$. (a) and (b) Plots of the RMSEs of $\hat{d}_2$ and $\hat{d}_3$, respectively. (c) and (d) Plots of the means of $\hat{d}_2$ and $\hat{d}_3$, respectively. Note that the IBBTDE failed in the estimation of $d_3$; therefore, its RMSEs are not displayed in (b).

with the associated two sensor measurements used, for different data lengths and overall SNRs. From Fig. 4, one can see that the MTDE algorithm performs better than the MTDE-1 algorithm due to the exploitation of space diversity by the former [see R9) and R10)]. One can also see that the proposed MTDE algorithm performs much better than the IBBTDE for lower SNR, whereas the latter performs better than the former for higher SNR. Furthermore, comparing Figs. 4 and 5, one can observe that the performances of the MTDE algorithm, the MTDE-1 algorithm, and the IBBTDE for Case B are worse than those for Case A. However, the proposed MTDE algorithm still works well for a wide range of overall SNR for Case B, justifying that the performance of the MTDE algorithm is less sensitive to the nonuniform $\text{SNR}_i$ among sensors because of space diversity gain, as mentioned in R9). On the other hand, the IBBTDE failed to estimate $d_3$ for Case B because the phase shift of $\pi$ (since $A_1 > 0$ and $A_3 < 0$) between the received measurements $y_1[n]$ and $y_3[n]$ is never considered in the model in [30], whereas the model given by (23) does.

## VI. Conclusion

Based on the relationship (see Fact 2) between the SIMO system and the optimal equalizer associated with the IFC for finite SNR, we have presented an FFT-based nonparametric blind SIMO system identification algorithm (i.e., the BSI algorithm) and an FFT-based TDE algorithm (i.e., the MTDE algorithm). As the conventional IFC-based methods, the proposed BSI algorithm also allows the unknown SIMO system to have common subchannel zeros and is thus more flexible than most SOS-based SIMO BSI methods. Moreover, some simulation results were provided to support that the proposed BSI algorithm outperforms the conventional IFC-based method. On the other hand, the proposed MTDE algorithm, which is robust against spatially correlated and coherent Gaussian noise and insensitive to the distribution of SNRs of sensors, can simultaneously estimate multiple time delays with space diversity exploited. The presented simulation results also support that the proposed TDE algorithm (i.e., the MTDE algorithm) with space diversity outperforms the IBBTDE (one of the conventional single-time-delay-based TDE approaches) for the case of nonuniform SNRs among sensors due to channel fading.

## Appendix A
## Proof of Property 1

The overall system associated with $\boldsymbol{H}'(\omega)$ given by (15) can be seen to be

$$G'(\omega) = \boldsymbol{V}^T(\omega)\boldsymbol{H}'(\omega) = G(\omega) \cdot e^{j(\omega\tau+\kappa)}. \tag{A.1}$$

Then, it can be established that

$$\begin{aligned} G'_p(\omega) &= \underbrace{(G'(\omega) \otimes G'(\omega) \otimes \cdots \otimes G'(\omega))}_{p-\text{term periodic convolution}} \\ &\quad \otimes \underbrace{(G'^*(-\omega) \otimes G'^*(-\omega) \otimes \cdots \otimes G'^*(-\omega))}_{(p-1)-\text{term periodic convolution}} \quad \text{[by (13)]} \end{aligned}$$

$$
\begin{aligned}
&= \left(\frac{1}{2\pi}\right)^{2p-2} \int_{-\pi}^{\pi} \cdots \int_{-\pi}^{\pi} G'(\theta_1) \ldots G'(\theta_p) \\
&\quad \cdot G'^*(-\theta_{p+1}) \ldots G'^*(-\theta_{2p-2}) \\
&\quad \cdot G'^* \left(-\omega + \sum_{k=1}^{2p-2} \theta_k\right) d\theta_1 \ldots d\theta_{2p-2} \\
&= \left(\frac{1}{2\pi}\right)^{2p-2} \cdot e^{j(\omega\tau+\kappa)} \int_{-\pi}^{\pi} \cdots \int_{-\pi}^{\pi} G(\theta_1) \ldots G(\theta_p) \\
&\quad \cdot G^*(-\theta_{p+1}) \ldots G^*(-\theta_{2p-2}) \\
&\quad \cdot G^* \left(-\omega + \sum_{k=1}^{2p-2} \theta_k\right) d\theta_1 \ldots d\theta_{2p-2} \quad \text{(by (A.1))} \\
&= e^{j(\omega\tau+\kappa)} \cdot \underbrace{(G(\omega) \otimes G(\omega) \otimes \cdots \otimes G(\omega))}_{p-\text{term periodic convolution}} \\
&\quad \otimes \underbrace{(G^*(-\omega) \otimes G^*(-\omega) \otimes \cdots \otimes G^*(-\omega))}_{(p-1)-\text{term periodic convolution}} \\
&= e^{j(\omega\tau+\kappa)} \cdot G_p(\omega). \qquad \text{(A.2)}
\end{aligned}
$$

Moreover, it can be shown, from (15), (A.2), and (11) that

$$G'_p(\omega) \cdot \boldsymbol{H}'^*(\omega) = G_p(\omega) \cdot \boldsymbol{H}^*(\omega) = \beta \cdot \boldsymbol{\mathcal{S}}_y^T(\omega) \boldsymbol{V}(\omega). \quad \text{(A.3)}$$

Thus, we have completed the proof. ■

## Appendix B
## Proof of Property 2

Because both $\mathbf{v}[n]$ and $\mathbf{h}[n]$ are stable $P \times 1$ linear time-invariant systems, the overall system $g[n] = \mathbf{v}^T[n]\mathbf{h}[n]$ is also a stable sequence. The zero phase of the stable overall system $g[n]$ implies that $G(\omega)$ is a continuous function of $\omega$ and

$$G(\omega) \geq 0, \quad \forall -\pi < \omega \leq \pi. \qquad \text{(B.1)}$$

By (A.2) with $\tau = \kappa = 0$, we obtain

$$
\begin{aligned}
G_p(\omega) &= \left(\frac{1}{2\pi}\right)^{2p-2} \int_{-\pi}^{\pi} \cdots \int_{-\pi}^{\pi} G(\theta_1) \ldots G(\theta_p) \\
&\quad \cdot G^*(-\theta_{p+1}) \ldots G^*(-\theta_{2p-2}) \\
&\quad \cdot G^* \left(-\omega + \sum_{k=1}^{2p-2} \theta_k\right) d\theta_1 \ldots d\theta_{2p-2} \\
&= \left(\frac{1}{2\pi}\right)^{2p-2} \int_{-\pi}^{\pi} \cdots \int_{-\pi}^{\pi} G(\theta_1) \ldots G(\theta_p) \\
&\quad \cdot G(-\theta_{p+1}) \ldots G(-\theta_{2p-2}) \\
&\quad \cdot G \left(-\omega + \sum_{k=1}^{2p-2} \theta_k\right) d\theta_1 \ldots d\theta_{2p-2} \\
&> 0, \quad \forall -\pi < \omega \leq \pi \quad \text{[by (B.1) and } \mathcal{A}4)]. \qquad \text{(B.2)}
\end{aligned}
$$

■

## Appendix C
## Proof of Property 3

For the sake of the proof, we need the following fact.

**Fact K1)** Assume that $a > 0, b > 0, c > 0$, and that $m$ is a positive integer. If $a(a^m + c^m) = b(b^m + c^m)$, then $a = b$.

The proof of Fact K1) is omitted here.

Let $\tilde{\mathbf{h}}[n]$ be an arbitrary system satisfying (11), and thus, we have

$$G_p(\omega)\boldsymbol{H}^*(\omega) = \tilde{G}_p(\omega)\tilde{\boldsymbol{H}}^*(\omega) = \beta \boldsymbol{\mathcal{S}}_y^T(\omega)\boldsymbol{V}(\omega). \qquad \text{(C.1)}$$

Without loss of generality, let us assume that both $G(\omega)$ and $\tilde{G}(\omega)$ are zero phase with positive $g[0]$ and $\tilde{g}[0]$, i.e.,

$$g[n] = g^*[-n], \quad \text{with } g[0] > 0 \qquad \text{(C.2)}$$

$$\tilde{g}[n] = \tilde{g}^*[-n], \quad \text{with } \tilde{g}[0] > 0. \qquad \text{(C.3)}$$

It can be obtained, from (C.1), that

$$\tilde{\boldsymbol{H}}(\omega) = \Gamma(\omega) \cdot \boldsymbol{H}(\omega) \qquad \text{(C.4)}$$

where

$$\Gamma(\omega) = \frac{G_p^*(\omega)}{\tilde{G}_p^*(\omega)} = \frac{G_p(\omega)}{\tilde{G}_p(\omega)} > 0 \quad \text{(by Property 2)} \qquad \text{(C.5)}$$

and that

$$
\begin{aligned}
&G_p(\omega)\boldsymbol{V}^H(\omega)\boldsymbol{H}^*(\omega) \\
&\quad = G_p(\omega)G^*(\omega) \\
&\quad = \tilde{G}_p(\omega)\boldsymbol{V}^H(\omega)\tilde{\boldsymbol{H}}^*(\omega) \\
&\quad = \tilde{G}_p(\omega)\tilde{G}^*(\omega) \geq 0 \quad \text{[by (C.1) and Property 2]}. \qquad \text{(C.6)}
\end{aligned}
$$

Let $s[n]$ be the inverse Fourier transform of $G_p(\omega)G^*(\omega)$, i.e.,

$$
\begin{aligned}
s[n] &= g_p[n] * g^*[-n] \\
&= \sum_{l=-\infty}^{\infty} |g[l]|^m g[l] g^*[l-n] \quad \text{[by (13)]} \qquad \text{(C.7)}
\end{aligned}
$$

where $m = 2(p-1)$, and $p \geq 2$. One can easily infer from (C.6) that

$$s[n] = \tilde{s}[n] \qquad \text{(C.8)}$$

where $s[n] = g_p[n] * g^*[-n]$, and $\tilde{s}[n] = \tilde{g}_p[n] * \tilde{g}^*[-n]$, as given by (C.7).

Let us further assume that $g[n] \neq 0$ only for $n \in [-L, L]$, and thus, $g_p[n] \neq 0$ only for $n \in [-L, L]$ by (13), and $s[n] \neq 0$ only for $n \in [-2L, 2L]$. Then, $s[n]$ given by (C.7) can be expressed as

$$
\begin{aligned}
s[n] &= \sum_{l=-L}^{L} |g[l]|^m g[l] g^*[l-n] \\
&\quad n = -2L, -2L+1, \ldots, 2L-1, 2L \qquad \text{(C.9)}
\end{aligned}
$$

and the equality $s[n] = \tilde{s}[n]$ implies that $\tilde{g}[n] \neq 0$ and $\tilde{g}_p[n] \neq 0$ only for $n \in [-L, L]$, and $\tilde{s}[n] \neq 0$ only for $n \in [-2L, 2L]$. Furthermore, it can be easily seen from (C.9) and (C.8) that

$$
\begin{aligned}
s[2L] &= |g[L]|^m g^2[L] \\
&= \tilde{s}[2L] = |\tilde{g}[L]|^m \tilde{g}^2[L] \qquad \text{(C.10)}
\end{aligned}
$$

■

which implies

$$g[L] = \tilde{g}[L] \quad \text{or} \quad g[L] = -\tilde{g}[L]. \tag{C.11}$$

Again, by (C.9), simplifying $s[2L-1] = \tilde{s}[2L-1]$ [by (C.8)] results in

$$g[L]g[L-1]\{|g[L]|^m + |g[L-1]|^m\} = \tilde{g}[L]\tilde{g}[L-1]\{|\tilde{g}[L]|^m + |\tilde{g}[L-1]|^m\}. \tag{C.12}$$

It can be easily shown from (C.11), (C.12), and Fact K1) (with $a = |g[L-1]|, b = |\tilde{g}[L-1]|$, and $c = |g[L]| = |\tilde{g}[L]|$) that

$$|g[L-1]| = |\tilde{g}[L-1]|. \tag{C.13}$$

Moreover, it can be inferred from (C.11)—(C.13) that

$$\frac{\tilde{g}[L-1]}{g[L-1]} = \frac{g[L]}{\tilde{g}[L]}. \tag{C.14}$$

By the same fashion, simplifying $s[n] = \tilde{s}[n]$ [by (C.8)] for $n = 2L-2, 2L-3, \ldots, L$, one can also prove, by (C.9) and Fact K1), that

$$|g[n]| = |\tilde{g}[n]|, \quad n = L, L-1, \ldots, 1, 0 \tag{C.15}$$

and

$$\frac{\tilde{g}[n]}{g[n]} = \frac{g[L]}{\tilde{g}[L]}, \quad n = L-1, L-2, \ldots, 1, 0 \tag{C.16}$$

which together with (C.11) leads to

$$g[n] = \tilde{g}[n], \quad \forall n \in [0, L] \quad (\text{since } g[0] > 0 \text{ and } \tilde{g}[0] > 0). \tag{C.17}$$

Moreover, one can infer from (C.2), (C.3), and (C.17) that

$$g[n] = \tilde{g}[n], \quad \forall n \in [-L, L]. \tag{C.18}$$

It can be easily seen from (C.18) and (13) that $G_p(\omega) = \tilde{G}_p(\omega)$, which gives rise to $\Gamma(\omega) = 1, \forall \omega$ [by (C.5)]. Therefore, one can obtain from (C.4) that

$$\tilde{\boldsymbol{H}}(\omega) = \boldsymbol{H}(\omega) \tag{C.19}$$

under the zero-phase assumption for both $g[n]$ and $\tilde{g}[n]$. Furthermore, by Property 1 and (C.19), $\boldsymbol{H}'(\omega) = \tilde{\boldsymbol{H}}(\omega) \cdot e^{j(\omega\tau+\kappa)} = \boldsymbol{H}(\omega) \cdot e^{j(\omega\tau+\kappa)}$ is also a solution of (11) under constraint C1). The assumption that $\tilde{g}[n] \neq 0$ only for $n \in [-L, L]$ can be relaxed by allowing $L \to \infty$. Thus, the proof has been completed. ■

## REFERENCES


[1] A. J. Paulraj and C. B. Padadias, "Space-time processing for wireless communications," *IEEE Signal Processing Mag.*, vol. 14, pp. 49–83, Nov. 1997.

[2] K. Abed-Meraim, W. Qiu, and Y. Hua, "Blind system identification," in *Proc. IEEE*, vol. 85, Aug. 1997, pp. 1310–1322.

[3] L. Tong and S. Perreau, "Multichannel blind identification: From subspace to maximum likelihood methods," in *Proc. IEEE*, vol. 86, Oct. 1998, pp. 1951–1968.

[4] Y. Hua, "Fast maximum likelihood for blind identification of multiple FIR channels," *IEEE Trans. Signal Processing*, vol. 44, pp. 661–672, Mar. 1996.

[5] C. L. Nikias and A. P. Petropulu, *Higher Order Spectral Analysis: A Nonlinear Signal Processing Framework*. Englewood Cliffs, NJ: Prentice-Hall, 1993.

[6] L. Tong, G. Xu, and T. Kailath, "A new approach to blind identification and equalization of multipath channels," in *Proc. 25th Asilomar Conf. Signals, Syst., Comput.*, vol. 2, Pacific Grove, CA, Nov. 4–6, 1991, pp. 856–860.

[7] E. Moulines, P. Duhamel, J.-F. Cardoso, and S. Mayrargue, "Subspace methods for the blind identification of multichannel FIR filters," *IEEE Trans. Signal Processing*, vol. 43, pp. 516–525, Feb. 1995.

[8] L. Perros-Meilhac, E. Moulines, K. Abed-Meraim, P. Chevalier, and P. Duhamel, "Blind identification of multipath channels: A parametric subspace approach," *IEEE Trans. Signal Processing*, vol. 49, pp. 1468–1480, July 2001.

[9] L. Tong and Q. Zhao, "Joint order detection and blind channel estimation by least squares smoothing," *IEEE Trans. Signal Processing*, vol. 7, pp. 2345–2355, Sept. 1999.

[10] Q. Zhao and L. Tong, "Adaptive blind channel estimation by least squares smoothing," *IEEE Trans. Signal Processing*, vol. 47, pp. 3000–3012, Nov. 1999.

[11] K. Abed-Meraim, E. Moulines, and P. Loubaton, "Prediction error methods for second-order blind identification," *IEEE Trans. Signal Processing*, vol. 45, pp. 694–705, Mar. 1997.

[12] J. K. Tugnait, "On blind identifiability of multipath channels using fractional sampling and second-order cyclostationary statistics," *IEEE Trans. Inform. Theory*, vol. 41, pp. 308–311, Jan. 1995.

[13] T. Endres, B. D. O. Anderson, C. R. Johnson, and L. Tong, "On the robustness of FIR channel identification from second-order statistics," *IEEE Signal Processing Lett.*, vol. 3, pp. 153–155, May 1996.

[14] H. Ali, J. H. Manton, and Y. Hua, "Modified channel subspace method for identification of SIMO FIR channels driven by a trailing zero filter bank precoder," in *Proc. IEEE Int. Conf. Acoust., Speech, Signal Process.*, vol. 4, Salt Lake City, UT, May 7–11, 2001, pp. 2053–2056.

[15] G. B. Giannakis, Y. Hua, P. Stoica, and L. Tong, *Signal Processing Advances in Wireless & Mobile Communications, Volume 1: Trends in Channel Estimation and Equalization*. Upper Saddle River, NJ: Prentice-Hall, 2001.

[16] D. Hatzinakos and C. L. Nikias, "Blind equalization using a tricepstrum based algorithm," *IEEE Trans. Commun.*, vol. 39, pp. 669–682, May 1991.

[17] D. H. Brooks and C. L. Nikias, "Multichannel adaptive blind deconvolution using the complex cepstrum of higher-order cross-spectra," *IEEE Trans. Signal Processing*, vol. 41, pp. 2928–2934, Sept. 1993.

[18] A. Swami, G. B. Giannakis, and S. Shamsunder, "Multichannel ARMA process," *IEEE Trans. Signal Processing*, vol. 42, pp. 898–913, Apr. 1994.

[19] J. K. Tugnait, "Parameter identifiability of multichannel ARMA models of linear non-Gaussian signals via cumulant matching," *IEEE Trans. Signal Processing*, vol. 43, pp. 3067–3069, Dec. 1995.

[20] ——, "Identification and deconvolution of multichannel linear non-Gaussian processes using higher order statistics and inverse filter criteria," *IEEE Trans. Signal Processing*, vol. 45, pp. 658–672, Mar. 1997.

[21] C.-Y. Chi, C.-H. Chen, and C.-Y. Chen, "Blind MAI and ISI suppression for DS/CDMA systems using HOS-based inverse filter criteria," *IEEE Trans. Signal Processing*, vol. 50, pp. 1368–1381, June 2002.

[22] C.-Y. Chi, C.-Y. Chen, C.-H. Chen, and C.-C. Feng, "Batch processing algorithms for blind equalization using higher-order statistics," *IEEE Signal Processing Mag.*, vol. 20, pp. 25–49, Jan. 2003.

[23] C.-Y. Chi and C.-H. Chen, "Cumulant based inverse filter criteria for blind deconvolution: Properties, algorithms, and application to DS/CDMA systems," *IEEE Trans. Signal Processing*, vol. 49, pp. 1282–1299, July 2001.

[24] C. H. Knapp and G. C. Carter, "The generalized correlation method for estimation of time delay," *IEEE Trans. Acoust., Speech, Signal Processing*, vol. ASSP-24, pp. 320–327, Aug. 1976.

[25] J. Ianniello, "Time delay estimation via cross-correlation in the presence of large estimation errors," *IEEE Trans. Acoust., Speech, Signal Processing*, vol. ASSP-30, pp. 998–1003, Dec. 1982.

[26] H.-H. Chiang and C. L. Nikias, "A new method for adaptive time delay estimation for non-Gaussian signals," *IEEE Trans. Signal Processing*, vol. 38, pp. 209–219, Feb. 1990.

[27] M. J. Hinich and G. R. Wilson, "Time delay estimation using the cross bispectrum," *IEEE Trans. Signal Processing*, vol. 40, pp. 106–113, Jan. 1992.

[28] J. K. Tugnait, "Time delay estimation with unknown spatially correlated Gaussian noise," *IEEE Trans. Signal Processing*, vol. 41, pp. 549–558, Feb. 1993.
[29] Y. Ye and J. K. Tugnait, "Time delay estimation using integrated polyspectrum," in *Proc. IEEE Int. Conf. Acoust., Speech, Signal Process.*, vol. 2, Adelaide, Australia, Apr. 19–22, 1994, pp. 397–400.
[30] ——, "Performance analysis of integrated polyspectrum based time delay estimators," in *Proc. IEEE Int. Conf. Acoust., Speech, Signal Process.*, vol. 5, Detroit, MI, May 9–12, 1995, pp. 3147–3150.
[31] S. M. Kay, *Modern Spectral Estimation*. Englewood Cliffs, NJ: Prentice-Hall, 1988.
[32] C.-H. Chen and C.-Y. Chi, "Two-dimensional Fourier series-based model for nonminimum-phase linear shift-invariant systems and texture image classification," *IEEE Trans. Signal Processing*, vol. 50, pp. 945–955, Apr. 2002.
[33] M. Jian, A. C. Kot, and M. H. Er, "Performance analysis of time delay estimation in a multi-path environment," in *Proc. IEEE 13th Int. Conf. Digital Signal Process.*, vol. 2, Santorini, Greece, July 2–4, 1997, pp. 919–922.
[34] Y.-C. Liang, A. R. Leyman, and B.-H. Soong, "Multipath time delay estimation using higher order statistics," in *Proc. IEEE Signal Processing Workshop Higher Order Statistics*, Banff, AB, Canada, July 21–23, 1997, pp. 9–13.
[35] Y. Liu, S.-X. Wang, Y.-C. Liang, and Z.-X. Li, "Multipath time delay estimation with unknown spatially correlated noise and multiple access interference using cyclic statistics," in *Proc. IEEE Conf. Decision Contr.*, vol. 4, Orlando, FL, Dec. 4–7, 2001, pp. 3338–3343.

**Chong-Yung Chi** (S'83–M'83–SM'89) was born in Taiwan, R.O.C., on August 7, 1952. He received the B.S. degree from the Tatung Institute of Technology, Taipei, Taiwan, in 1975, the M.S. degree from the National Taiwan University, Taipei, in 1977, and the Ph.D. degree from the University of Southern California, Los Angeles, in 1983, all in electrical engineering.

From July 1983 to September 1988, he was with the Jet Propulsion Laboratory, Pasadena, CA, where he worked on the design of various spaceborne radar remote sensing systems including radar scatterometers, SARs, altimeters, and rain mapping radars. From October 1988 to July 1989, he was a visiting specialist at the Department of Electrical Engineering, National Taiwan University. He has been a Professor with the Department of Electrical Engineering, National Tsing University, Hsinchu, Taiwan, since August 1989, where he has also been the Chairman of Institute of Communications Engineering since August 2002. He was a visiting researcher with the Advanced Telecommunications Research (ATR) Institute International, Kyoto, Japan, between May and June 2001. He has published more than 110 technical papers in radar remote sensing, system identification and estimation theory, deconvolution and channel equalization, digital filter design, spectral estimation, and higher order statistics (HOS)-based signal processing. His research interests include signal processing for wireless communications, statistical signal processing, and digital signal processing and their applications. He is an Editorial Board Member of the *EURASIP Journal on Applied Signal Processing*.

Dr. Chi is an active member of the Society of Exploration Geophysicists, a member of the European Association for Signal Processing, and an active member of the Chinese Institute of Electrical Engineering. He was a technical committee member of both the 1997 and 1999 IEEE Signal Processing Workshop on Higher Order Statistics (HOS) and the 2001 IEEE Workshop on Statistical Signal Processing (SSP). He was also a member of International Advisory Committee of TENCON 2001 and a member of International Program Committee of the Fourth International Symposium on Independent Component Analysis and Blind Source Separation (ICA-2003). He was a co-organizer and a general co-chairman of 2001 IEEE SP Workshop on Signal Processing Advances in Wireless Communications (SPAWC-2001), the International Liaison of SPAWC-2003, and Technical Committee Member and International Liaison (Asia and Australia) of SPAWC-2004. He was a Program Committee Member of the International Conference on Signal Processing (ICSP-2003) and a Technical Committee Member of the Third IEEE International Symposium on Signal Processing and Information Technology (ISSPIT'03). He was also the Chair of Information Theory Chapter of IEEE Taipei Section from July 2001 to August 2003. Currently, he is an Associate Editor for the IEEE TRANSACTIONS ON SIGNAL PROCESSING.

**Ching-Yung Chen** was born in Taiwan, R.O.C., on November 14, 1975. He received the B.S. and Ph.D. degrees from the Department of Electrical Engineering, National Tsing Hua University, Hsinchu, Taiwan, in 1997 and 2003, respectively.

Since October 2003, he has been with the Computer and Communications Research Laboratories, Industrial Technology Research Institute, Hsinchu, where he works in the Transmission Technology Department, Digital Video and Optical Communications Technologies Division, for the design, analysis, and implementation of the receiver in digital video broadcasting (DVB) systems. His research interests include statistical signal processing, digital signal processing, wireless communications, and DVB systems.

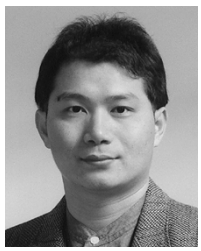

**Chii-Horng Chen** was born in Taiwan, R.O.C., on December 2, 1970. He received the B.S. degree from the Department of Control Engineering, National Chiao Tung University, Hsinchu, Taiwan, in 1992 and the Ph.D. degree from the Department of Electrical Engineering, National Tsing Hua University, Hsinchu, Taiwan, in 2001.

Since October 2001, he has been with ADMtek Incorporated, Hsinchu, where he works on the analysis, design, and implementation of the transceiver of wireless local area networks. His research interests include wireless communications, statistical signal processing, and digital signal processing.

**Chih-Chun Feng** (S'97–M'99) received the B.S. degree in electronic engineering from Feng Chia University, Taichung, Taiwan, R.O.C., in 1992, the M.S. degree in communication engineering from National Chiao Tung University, Hsinchu, Taiwan, in 1994, and the Ph.D. degree in electrical engineering from National Tsing Hua University, Hsinchu, in 1999.

In 2001, he joined Computer and Communications Research Laboratories (CCL), Industrial Technology Research Institute (ITRI), Hsinchu, where he is currently a Section Manager with the Transmission Technology Department, Digital Video and Optical Communications Technologies Division. His current research interests are in the areas of digital signal processing, wireless communications, and digital broadcasting technologies.

**Chun-Hsien Peng** was born in Taiwan, R.O.C., on November 21, 1978. He received the B.S. degree from the Department of Electrical Engineering, National Taipei University of Technology, Taipei, Taiwan, in 2001, and is currently pursuing the Ph.D. degree with the Institute of Communications Engineering, Department of Electrical Engineering, National Tsing Hua University, Hsinchu, Taiwan.

His research interests include statistical signal processing, digital signal processing, and wireless communications.